

Supporting Information: Ilgen et al., “Switching on” iron in clay minerals

Supporting Information

“Switching on” iron in clay minerals

A.G. Ilgen^{1*}, R.K Kukkadapu², K. Leung¹, and R.E. Washington¹

1. Sandia National Laboratories, Geochemistry Department, 1515 Eubank SE Mailstop 0754, Albuquerque, NM 87185-0754, United States
2. Pacific Northwest National Laboratory, Environmental Molecular Sciences Laboratory, Richland, WA, United States

*Corresponding author. E-mail agilgen@sandia.gov

Pages: 9
Figures: 4
Tables: 3

X-ray absorption spectroscopy (XAS) data analysis

We used X-ray absorption spectroscopy to quantify the oxidation state of iron, and its local chemical environment in the native and activated nontronite NAu-1. XAS data and shell-by-shell fits are shown in Figure S1. The modeling results indicate that Fe(III) resides in octahedral lattice sites in both activated and native nontronites. The 1st shell Fe-O distance is characteristic of octahedrally-coordinated iron, ($2.06 \pm 0.01 \text{ \AA}$), and there is no evidence for any tetrahedral Fe. The Fe-Fe backscattering at $3.10 (\pm 0.06) \text{ \AA}$ is characteristic for the edge-sharing iron octahedra. The shell-by-shell fitting results are summarized in Table S1. After the activation treatment, we observe a subtle increase in the magnitude of the Fe-Fe backscattering shell at $3.11 \pm 0.06 \text{ \AA}$ and Fe-O shell at $3.75 \pm 0.05 \text{ \AA}$. We interpret this change as local migration of some of the iron atoms into di-octahedral vacancies, and forming tri-octahedral domains, as has been reported earlier.¹

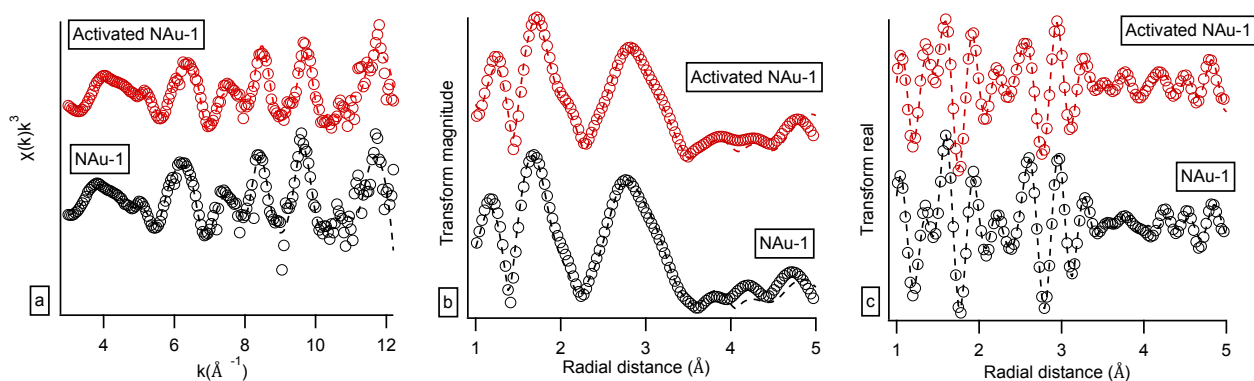


Figure S1. XAFS data (open circles) and fits (dashed lines) of Fe K-edge XAFS collected for natural nontronite NAu-1 in its native form and after the surface activation treatment: (a) EXAFS $\chi(k)k^3$ data; (b) magnitude of Fourier transform of EXAFS $\chi(k)k^3$ data, uncorrected distances; (c) Fourier transform of EXAFS $\chi(k)k^3$ data plotted in real space, uncorrected distances. Fitting parameters are summarized in Table S1.

Table S1. Summary of extended X-ray absorption fine structure spectroscopy (XAFS) shell-by-shell fitting results. Fitting was done in R-space; k-weights of 1, 2, and 3 were fitted simultaneously, the amplitude reduction factor S_0 was 0.79. Error at a 95 % confidence level is shown in parenthesis.

Sample	¹⁾ k-range	R-range (Å)	Shell	²⁾ CN	³⁾ R (Å)	⁴⁾ σ^2 (Å ²)	⁵⁾ ΔE_0 eV	⁶⁾ R-factor	⁷⁾ Red χ^2	⁸⁾ Ind. Pts.
Native nontronite N Au-1	2.7-12.0	1.3-5.0	Fe-O	5.1(5)	2.06(1)	0.001(1)	7(1)	0.02	8.5	29
			Fe-O	3(2)	2.40(8)	0.004*				
			Fe-Fe	5.6(6)	3.10(6)	0.003(1)				
			Fe-Si	3(1)	3.64(4)	0.001(4)				
			Fe-O	1.4(6)	3.72(4)	0.004*				
			Fe-Si	2(2)	4.52(8)	0.009(1)				
Activated nontronite N Au-1	2.7-12.0	1.3-5.0	Fe-O	5.7(8)	2.07(1)	0.004(1)	12(1)	0.02	34	29
			Fe-O	3(1)	2.40(3)	0.003(3)				
			Fe-Fe	5.9(8)	3.11(1)	0.005(1)				
			Fe-Si	2(1)	3.67(4)	0.002(4)				
			Fe-O	5(1)	3.73(5)	0.01(1)				
			Fe-Si	3(2)	4.52(6)	0.004*				
			Fe-Fe	10(4)	5.35(4)	0.01(1)				

¹ Usable k-range

² Coordination number

³ Bond length

⁴ Debye-Waller factors: mean-square amplitude reduction factor, including thermal and static disorder components

⁵ Energy shift between the theoretical and measured spectrum

$$R_{factor} = \frac{\sum_i (data_i - fit_i)^2}{\sum_i data_i^2}$$

⁶ R-factor (mean square misfit)

$$\chi_v^2 = \frac{N_{idp}}{N_{pts}} \sum_i \left(\frac{data_i - fit_i}{\varepsilon_i} \right)^2 / (N_{idp} - N_{var})$$

⁷ Reduced chi-square

⁸ Independent points (number of data points minus number of variable parameters)

$$N_{idp} = N_{pts} - N_{var}$$

* Constrained Debye-Waller factors

Modeling of Mössbauer spectra

The details about Mössbauer spectroscopy findings are in the main text. Below we provide additional tables and figures. In Table S2 we show the fractions of different iron species and the average calculated oxidation state of activated nontronite and activated nontronite reacted with As(III) for 2 weeks. Voigt-based structural fitting routine was used for Mössbauer data analysis.² In Figure S2 we show data for non-activated nontronite NAu-1, which illustrates that no Fe(II) was present prior to the partial reduction treatment, and no Fe(III)-oxide impurities were present in our samples. With the signal-to-noise ratios of our spectra, the detection limit for Fe(II) is within 1-2% of total Fe in nontronite. In Table S3 and Figure S3 we show alternative fitting models, not included in the main text. These alternative models further confirm that optimal fit for room temperature Mössbauer data is achieved with two Fe(III) doublets, Fe(III)-1 and Fe(III)-1', and for 12 K feature—with one Fe(III) doublet that is a composite of Fe(III)-1, Fe(III)-1', and Fe(III)-2 (shown in Figure 3 and summarize in Table 2 in the main text).

Table S2. Fractions of different Fe species, and the average charge of mixed-Fe(II)/Fe(III) signal in room temperature (273 K) Mössbauer spectra.

Sample	Fe(II)-1 %	Fe(III)-1 + Fe(III)-1' %	Fe-edge ¹ %	Total Fe(II) %	Calc ² Fe(II)-edge %	Calc ³ Fe(III)- edge %	Fraction ⁴ of Fe(II)-edge	Fraction ⁵ of Fe(III)-edge	Average ⁶ oxidation state Fe-edge
Activated	12.43	69.5	18.0	26.33	13.9	4.1	0.77	0.23	2.23
Activated+ As (III), 2 weeks	18.53	69.6	11.88	29.71	11.18	0.7	0.94	0.06	2.06

Notes:

¹ The percentage of iron contribution from the edge sites (Fe(II)-2+Fe(III)-2).

² Calculated as the difference between the total Fe(II) (12 K) and the Fe(II)-1 (RT).

³ Calculated as the difference between the Fe-edge % and calculated Fe(II)-edge %.

⁴ Calculated fraction of Fe(II) at the edge sites; calculated as $\frac{\text{Calc Fe(II)edge}}{[\text{Calc Fe(II)edge} + \text{Calc Fe(III)edge}]}$

⁵ Calculated fraction of Fe(III) at the edge sites; calculated as $\frac{\text{Calc Fe(III)edge}}{[\text{Calc Fe(II)edge} + \text{Calc Fe(III)edge}]}$

⁶ Average oxidation state of iron at the edge sites; calculated as
 $[Fraction\ of\ Fe(II)edge] \times 2 + [Fraction\ of\ Fe(III)edge] \times 3$

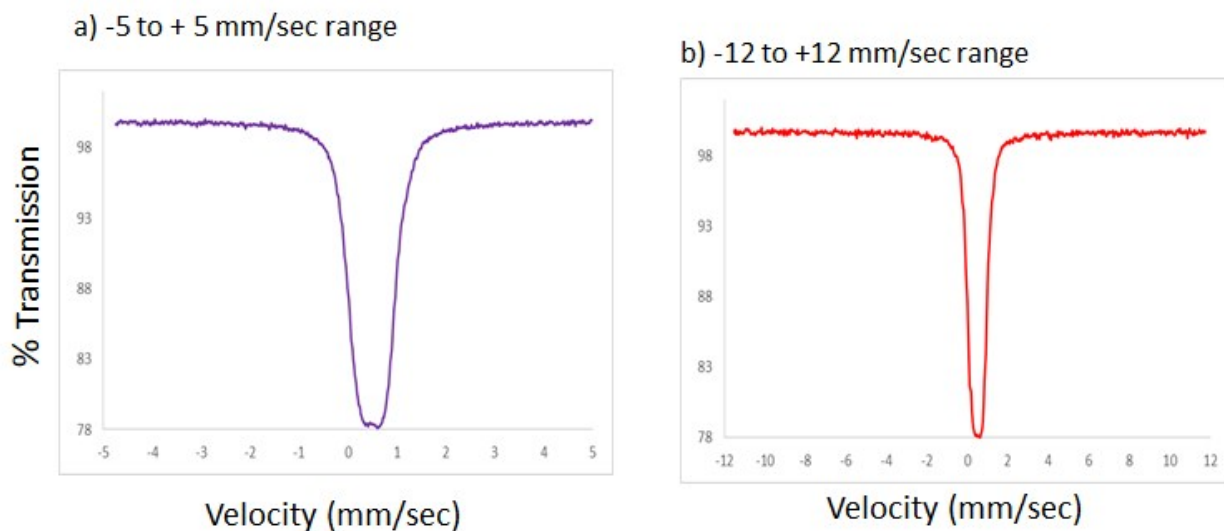


Figure S2. ⁵⁷Fe-Mössbauer spectra collected on raw nontronite N Au-1 at 12K. (a) Peaks due to Fe(II) are absent (high-energy doublet peak is expected between +2.5 mm and +3.1 mm/sec), (b) Sextet peaks due to Fe(III)-oxide are absent (peaks are expected between -10 to +10 mm/sec region)t.

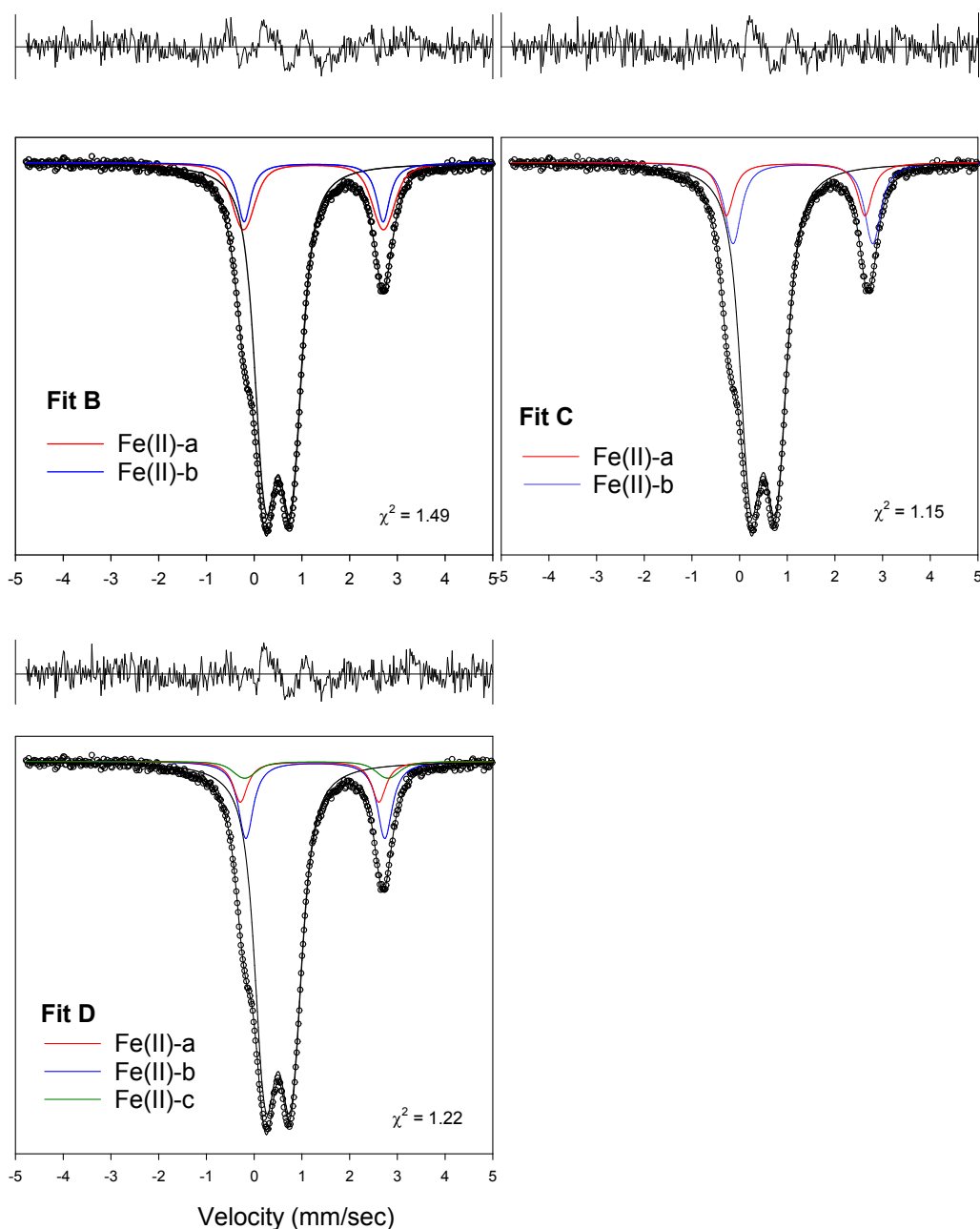


Figure S3. Mössbauer spectra of activated sample at 12 K modeled with multiple Fe(II) doublets, instead of one Fe(II) (Figure 3b of main section – referred as Fit A); a) and b) 12 K spectrum modeled with two different Fe(II) doublets of varying relative intensities and Mössbauer parameters – Fit B and Fit C, and c) a 12 K modeled spectrum with 3 different Fe(II) doublets of different relative intensities and Mössbauer parameters – Fit D. T

Table S3. Alternative fitting models for 12 K Mössbauer spectra for activated nontronite N Au-1.

Activated N Au-1	HWHM ^a	χ^2 ^b	Type ^c	<CS> ^d	<D> ^e	σ_{Δ} ^f	area % ^g	Notes
------------------	-------------------	-----------------------	-------------------	-------------------	------------------	--------------------------------	---------------------	-------

Supporting Information: Ilgen et al., “Switching on” iron in clay minerals

	mm/sec			mm/sec	mm/sec	mm/sec	(2 σ std dev)	
Fit B	0.17	1.49	Fe(II)-a	1.24	2.93	0.3	16.7(22)	1
[2 Fe(II) - fit]			Fe(II)-b	1.25	2.91	0.0004	10.3(22)	2
							Fe(II)-total, 27%	
			Fe(III)	0.5	0.53	0.53	73.0 (26)	3
Fit C	0.19	1.15	Fe(II)-a	1.29	2.92	0.1	16(31)	4
[2 Fe(II) - fit]			Fe(II)-b	1.18	2.91	0.0003	10(33)	5
							Fe(II)-total, 26%	
			Fe(III)	0.5	0.53	0.24	74(38)	
Fit D	0.18	1.22	Fe(II)-a	1.28	2.91	0.06	15(30)	6
[3 Fe(II) - fit]			Fe(II)-b	1.16	2.9	6.00E-05	8(31)	7
			Fe(II)-c	1.3	3	0.3	4.4(32)	8
							Fe(II)-total, 27.4%	
			Fe(III)	0.5	0.53	0.25	73(35)	

^a Lorentzian peak width - half-width and half maxima; ^b Goodness of fit; ^c Type of Fe species; ^d Center shift; ^e Quadrupole splitting; ^f Standard deviation of Δ ; ^g Peak area.
No coupling is allowed between CS and Δ .

Notes:

1. Fe(II) parameters similar to edge-Fe(II) species reported in Neumann et al., 2013.³
2. Higher standard deviation, compared to the Fit A reported in the main text (Figure 3 in the manuscript).
3. Higher value for the goodness of fit (worse fit), compared to the Fit A reported in the main text (Figure 3 in the manuscript).
4. Fe(II)-b parameters are lower, compared to those reported for edge-site Fe(II) in Neumann et al., 2013.³
5. Unrealistic standard deviation values for spectral area.
6. Fe(II)-b parameters are lower than, compared to those reported in in Neumann et al., 2013.³
7. Fe(II)-c parameters are lower than those reported for basal Fe(II) in Neumann et al., 2013.³
8. Unrealistic standard deviation values for spectral area.

Diffuse reflectance (DR) spectroscopy to track the Fe^{II}-O-Fe^{III} moiety *in situ*

We tested how the addition of Fe²⁺ to the nontronite N_{Au}-1 suspension affects the diffuse reflectance spectral features. As discussed in the main text, diffuse reflectance spectra is indicative of the Fe(II)↔Fe(III) intervalence electron transfer in nontronite samples.⁴ We observed a broad peak, which was seen in nontronite suspensions only when Fe(II) was present. Iron (II) was introduced into the clay mineral structure by either partial reduction treatment, or by the addition of aqueous Fe²⁺. At the pH 7.0 ± 0.1, Fe²⁺ adsorbs onto the edge sites of nontronite, and Fe^{II}-O-Fe^{III} moieties are formed at the edge sites. The suspensions with native nontronite N_{Au}-1 were spiked with FeCl₂ in an anaerobic glove box, and then DR spectra were collected 15 minutes, 1 hour, and 24 hours after the addition. The results are shown in Figure S4. A broad peak at ~720 nm is observed for N_{Au}-1 suspensions with added Fe²⁺, and not observed for the nontronite suspension without the added Fe²⁺. This is due to Fe²⁺ adsorbing at the edge sites of nontronite surfaces and forming the Fe^{II}-O-Fe^{III} moieties (Fe_{2.5+} domains), necessary for the rise of this spectral feature. When the integrated area of the peak is plotted as a function of the added Fe²⁺ concentration, the curve has a shape of an adsorption isotherm (Figure S4). The adsorption isotherm is consistent between 15 minutes, 1 hour, and 24 hours, indicating that adsorption equilibrium is achieved within minutes.

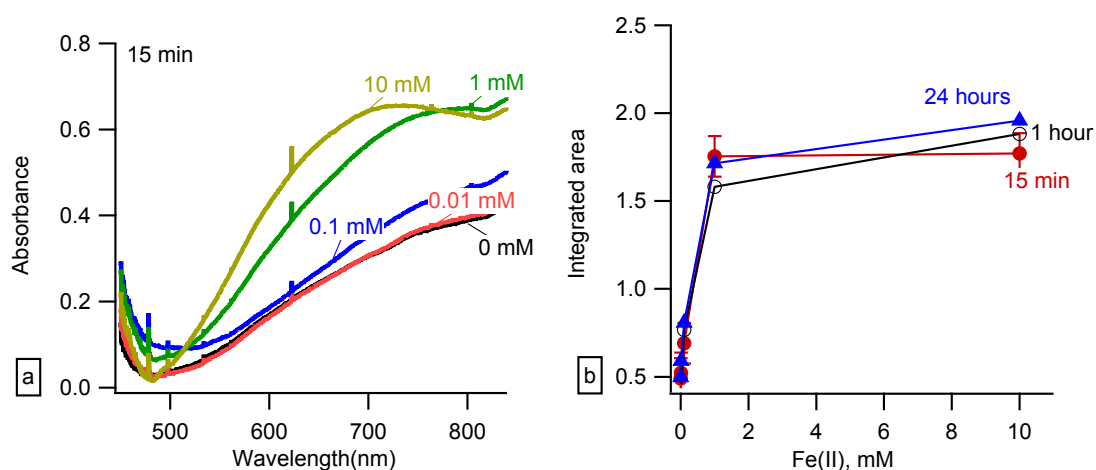


Figure S4. Diffuse reflectance data collected on native

nontronite N_{Au}-1 suspensions with and without the addition of aqueous Fe²⁺; (a) Absorbance spectra of clay mineral suspensions under anoxic conditions following the addition of Fe²⁺. Spectra were collected 15 minutes after Fe²⁺ was added to the clay mineral suspensions; (b) The average integrated area of the 720-nm peak vs. the concentration of Fe²⁺ for N_{Au}-1. Spectra

were collected 15 minutes, 1 hour, and 24 hours after Fe²⁺ was added to the clay mineral suspensions.

References

- 1 Manceau, A. *et al.* Oxidation-reduction mechanism of iron in dioctahedral smectites: I. Crystal chemistry of oxidized reference nontronites. *Am. Mineral.* **85**, 133-152 (2000).
- 2 Rancourt, D. & Ping, J. Voigt-based methods for arbitrary-shape static hyperfine parameter distributions in Mössbauer spectroscopy. *Nuclear Instruments and Methods in Physics Research Section B: Beam Interactions with Materials and Atoms* **58**, 85-97 (1991).
- 3 Neumann, A., Olson, T. L. & Scherer, M. M. Spectroscopic evidence for Fe (II)–Fe (III) electron transfer at clay mineral edge and basal sites. *Environ. Sci. Technol.* **47**, 6969-6977 (2013).
- 4 Merola, R. B., Fournier, E. D. & McGuire, M. M. Spectroscopic investigations of Fe²⁺ complexation on nontronite clay. *Langmuir* **23**, 1223-1226 (2007).